Computational and Applied Mathematics (2020) 39:8
https://doi.org/10.1007/s40314-019-0986-2

On the graphene Hamiltonian operator

C. Conca[1] · R. Orive[2,3] · J. San Martín[1] · V. Solano[4,5]

Received: 29 January 2019 / Revised: 14 September 2019 / Accepted: 13 October 2019 /
Published online: 26 October 2019

Abstract
We solve a second-order elliptic equation with quasi-periodic boundary conditions defined on a honeycomb lattice that represents the arrangement of carbon atoms in graphene. Our results generalize those found by Kuchment and Post (Commun Math Phys 275(3):805–826, 2007) to characterize not only the stability but also the instability intervals of the solutions. This characterization is obtained from the solutions of the energy eigenvalue problem given by the lattice Hamiltonian. We employ tools of the one-dimensional Floquet theory and specify under which conditions the one-dimensional theory is applicable to the structure of graphene. The systematic study of such stability and instability regions provides a tool to understand the propagation properties and behavior of the electrons wavefunction in a hexagonal lattice, a key problem in graphene-based technologies.

Keywords Periodic solutions · General spectral theory · Spectral theory and eigenvalue problems · Graphene · Honeycomb structure

Communicated by Jose Alberto Cuminato.

✉ V. Solano
vsolano@udd.cl

C. Conca
cconca@dim.uchile.cl

R. Orive
rafael.orive@icmat.es

J. San Martín
jorge@dim.uchile.cl

1 Mathematical Engineering Department, Center for Mathematical Modeling-UMI 2807 CNRS-UChile and Center for Biotechnology and Bioengineering, Universidad de Chile, Beauchef 851, Santiago, Chile

2 Mathematics Department, Science Faculty, Universidad Autónoma de Madrid, 28049 Madrid, Spain

3 Instituto de Ciencias Matemáticas ICMAT (CSIC-UAM-UC3M-UCM), Nicolás Cabrera, 13-15, 28049 Madrid, Spain

4 Mathematical Engineering Department and Center for Mathematical Modeling UMI 2807 CNRS-UChile, Universidad de Chile, Beauchef 851, Santiago, Chile

5 Engineering Faculty, Universidad del Desarrollo, Avenida La Plaza 700, Santiago, Chile

Mathematics Subject Classification 34L05 · 82D80 · 34B60 · 34B45 · 47A10 · 34D20

1 Introduction

Graphene is a honeycomb lattice of carbon atoms. Recently, it has attracted a lot of attention due to its peculiar electronic and mechanical properties and broad range of applications (Harris 2002; Katsnelson 2007; Kuchment and Post 2007; Saito et al. 1998). To predict and understand this properties, mathematical models are not only useful but necessary. This problem has been approached from different scientific fields such as quantum networks (e.g., Amovilli et al. 2004; Korotyaev and Lobanov 2007, 2006; Leys et al. 2004), also called quantum graphs, in chemistry (Pauling 1936; Ruedenberg and Scherr 1953) and physics (Alexander 1983; Avron et al. 1988; De Gennes 1981; Mills and Montroll 1970; Montroll 1970) (see also Kuchment 2002, 2004 and references therein). The characterization of the dispersion relation of the honeycomb lattice is of particular interest for exploiting graphene electronic properties. This is obtained from the solution of the energy eigenvalue problem given by the lattice Hamiltonian. A method to completely characterize the set of solutions is to divide its analysis in stability and instability intervals, previously done for a one-dimensional system in $\mathbb{R}$ (Allaire and Orive 2005).

We will present the graphene G defined as a graph, i.e., with its respective components: a set of vertices $\mathcal{V}$ and a set of edges $\mathcal{A}$. Then we will define two spaces in the geometrical basis G, $L^2(G)$ and $H^2(G)$, that allow us to solve the Hamiltonian in the edges of G as $\mathcal{H} : H^2(G) \subset L^2(G) \to L^2(G)$. Thus, the functions $\Psi = (\Psi_a)_{a\in\mathcal{A}}$ such that $\mathcal{H}\Psi = \lambda\Psi$ have to satisfy the following conditions:

(i) $\sum_{a\in\mathcal{A}} \|\Psi_a\|^2_{H^2(a)} < \infty$.
(ii) For all $v \in \mathcal{V}$, for all $a_1, a_2 \in \mathcal{A}$, $[\boldsymbol{v} \in a_1 \cap a_2 \Rightarrow \Psi_{a_1}(\boldsymbol{v}) = \Psi_{a_2}(\boldsymbol{v})]$ (continuity condition).
(iii) For all $\boldsymbol{v} \in \mathcal{V}$, $\sum_{\substack{\boldsymbol{v}_2\in\mathcal{V} \\ [\boldsymbol{v},\boldsymbol{v}_2]\in\mathcal{A}}} D\Psi_{[\boldsymbol{v},\boldsymbol{v}_2]}(\boldsymbol{v}; \boldsymbol{v}_2 - \boldsymbol{v}) = 0$, where $D\Psi_{[\boldsymbol{v},\boldsymbol{v}_2]}(\boldsymbol{v}; \boldsymbol{v}_2 - \boldsymbol{v})$ is the directional derivative of the function $\Psi_{[\boldsymbol{v},\boldsymbol{v}_2]}$ at the point$\boldsymbol{v}$ in the direction of $[\boldsymbol{v}_2 - \boldsymbol{v}]$ (flow condition).

From these special and particular conditions, we will obtain the important results presented in this paper. We completely characterize the stability and instability intervals of a energy eigenvalues problem in a honeycomb lattice G, showing the versatility of this approach. However, remarkable difference is present in the structure of the stability regions raising from the more complex structure of graphene-like systems.

The paper is structured as follows. Section 2 explains the results known as Floquet Theory applied to our particular case as it is developed in Allaire and Orive (2005). In Sect. 3, the graphene G is defined geometrically. Section 4 shows how the Hamiltonian operator $\mathcal{H}$ acts through G and the parametrization that allows us to identify each edge with the segment $[0, 1]$. From the given theoretical frame, in Sect. 5, we look for a characterization of the functions $\Psi = (\Psi_a)_{a\in\mathcal{A}}$ that satisfies the conditions of continuity and flow (ii)–(iii). To analyze the graphene spectrum, in Sect. 6, we study the functions Ψ that satisfies such conditions, along with the eigenvalue equation $\mathcal{H}\Psi = \lambda\Psi$ and properties of quasi-periodicity. Finally, we determine for which values of λ these solutions are bounded or unbounded, analyzing the respective dispersion relation.

2 Theoretical framework

We will center our analysis in the result shown by Allaire and Orive in Allaire and Orive (2005), where the authors propose to find the stability and instability intervals of a second-order elliptic equation on the real line with periodic coefficients (Hill's equation). They introduced a new family of non-self-adjoint operators, formally equivalent to the Bloch ones (Bloch 1929; Conca 1995) but with an imaginary Bloch parameter, that they call exponential, proving that the problem admits a countable infinite number of eigenvalues which, when they are real, completely characterize the intervals of instability of Hill's equation.

The closure of the stability intervals are called *Bloch bands* and the non-empty open intervals between two Bloch bands are called *gaps*.

2.1 The Bloch spectrum

Let us consider the Hill's equation defined in Eastham (1973) as

$$-u''(x) + V(x)u(x) = \lambda u(x). \tag{1}$$

Here, the function V is real, piecewise-continuous and 1-periodic. We know that Eq. (1) has a basis of two linearly independent solutions $\varphi_1(\cdot;\lambda)$ and $\varphi_2(\cdot;\lambda)$, functions of the parameter λ, that satisfy

$$\varphi_1(0;\lambda) = 1,\ \varphi_1'(0;\lambda) = 0,\ \varphi_2(0;\lambda) = 0,\ \varphi_2'(0;\lambda) = 1. \tag{2}$$

It is clear that any solution u of (1) can be written as a linear combination:

$$u(x) = u(0)\varphi_1(x;\lambda) + u'(0)\varphi_2(x;\lambda). \tag{3}$$

The *discriminant* of (1) is given by

$$\mathcal{D}(\lambda) = \varphi_1(1;\lambda) + \varphi_2'(1;\lambda).$$

If the function V satisfies the symmetry relation $V(1-x) = V(x)$, then

$$\varphi_2'(1;\lambda) = \varphi_1(1;\lambda), \tag{4}$$

implying

$$\mathcal{D} = 2\varphi_1(1;\lambda). \tag{5}$$

Furthermore, when we restrict ourselves to $\lambda \in \mathbb{R}$ (and since all coefficients in (1) are real valued), it is possible to classify the solutions of (1): a solution is said to be *stable* if it is uniformly bounded, and *unstable* if it is unbounded. According to Conca (1995) and Eastham (1973), there exist a countably infinite sequence $\{\alpha_n\}_{n\in\mathbb{N}}$ of real roots of $\mathcal{D}(\lambda) = 2$ and a countably infinite sequence $\{\beta_n\}_{n\in\mathbb{N}}$ of real roots of $\mathcal{D}(\lambda) = -2$ such that

$$\cdots < \alpha_0 < \beta_0 \leq \beta_1 < \alpha_1 \leq \alpha_2 < \beta_2 \leq \beta_3 < \alpha_3 \leq \alpha_4 < \cdots$$

(see Fig. 1). The collection of disjoint open intervals

$$]\alpha_0, \beta_0[,\ ]\beta_1, \alpha_1[,\ ]\alpha_2, \beta_2[,\ ]\beta_3, \alpha_3[,\ \cdots$$

is called the *stability intervals* of (1) and their union

$$S =]\alpha_0, \beta_0[\cup]\beta_1, \alpha_1[\cup]\alpha_2, \beta_2[\cup]\beta_3, \alpha_3[\cup \cdots$$

is called the *region of stability*. Analogously,

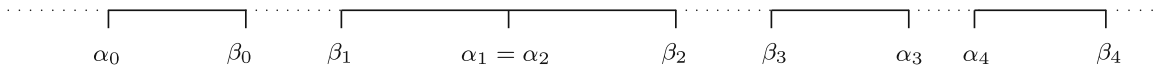

Fig. 1 The numbers α_n and β_n organized in stability and instability intervals

$$U =]-\infty, \alpha_0[\cup]\beta_0, \beta_1[\cup]\alpha_1, \alpha_2[\cup]\beta_2, \beta_3[\cup \cdots$$

is called the *region of instability*. In consequence, $|\mathcal{D}(\lambda)| < 2$ for $\lambda \in S$, and $|\mathcal{D}(\lambda)| > 2$ for $\lambda \in U$.

In addition, from the Floquet's Theory (Eastham 1973), we have

(i) For $\lambda \in U$, there exists $\theta \in \mathbb{R}\backslash\{0\}$ such that (1) has two linearly independent solutions of the type $e^{\theta x} p_1(x)$ and $e^{-\theta x} p_2(x)$, with p_1, p_2 1-periodic and characteristic multipliers $\rho_1 = e^{\theta}$ and $\rho_2 = e^{-\theta}$; or, with p_1, p_2 semi-periodic and characteristic multipliers $\rho_1 = -e^{\theta}$ and $\rho_2 = -e^{-\theta}$.

(ii) For $\lambda \in S$, there exists $\theta \in]0, \pi[$, or $\theta \in]-\pi, 0[$, such that (1) has two linearly independent solutions of the type $e^{i\theta x} p_1(x)$ and $e^{-i\theta x} p_2(x)$, with p_1, p_2 1-periodic and characteristic multipliers $\rho_1 = e^{i\theta}$ and $\rho_2 = e^{-i\theta}$.

(iii) If $\alpha_{2k+1} = \alpha_{2k+2}$, then for $\lambda = \alpha_{2k+1} = \alpha_{2k+2}$, Eq. (1) has two linearly independent solutions p_1 y p_2 1-periodic. If $\alpha_{2k+1} < \alpha_{2k+2}$, then for $\lambda = \alpha_{2k+1}$ and for $\lambda = \alpha_{2k+2}$, Eq. (1) has two linearly independent solutions of the type $p_1(x)$ and $xp_1(x) + p_2(x)$, with p_1 and p_2 1-periodic.

(iv) If $\beta_{2k} = \beta_{2k+1}$, then for $\lambda = \beta_{2k} = \beta_{2k+1}$, Eq. (1) has two linearly independent solutions p_1 y p_2 semi-periodic. If $\beta_{2k} < \beta_{2k+1}$, then for $\lambda = \beta_{2k}$ and for $\lambda = \beta_{2k+1}$, Eq. (1) has two linearly independent solutions of the type $p_1(x)$ and $xp_1(x) + p_2(x)$, with p_1 and p_2 semi-periodic.

We recall other classical results of a theory on the eigenvalue structure of (1), known as the *Bloch Decomposition Theory* (Aguirre and Conca 1988; Conca and Vanninathan 1997). If we consider (1) as a spectral problem in $L^2(\mathbb{R})$, it is a natural question to determine its spectrum. To this end, we consider the following Bloch spectral problem parameterized by $\theta \in \mathbb{R}$:

$$\begin{cases} \text{Find } \lambda = \lambda(\theta) \in \mathbb{R} \text{ and } \Psi = \Psi(x, \theta); \\ -\Psi''(x, \theta) + V(x)\Psi(x, \theta) = \lambda(\theta)\Psi(x, \theta) \ \text{ in } \mathbb{R} \\ \Psi(x + 1, \theta) = e^{i\theta}\Psi(x, \theta), \quad \forall x. \end{cases} \tag{6}$$

It is well known that for each $\theta \in]-\pi, \pi]$, the above spectral problem (6) admits a discrete sequence of eigenvalues with the following properties

$$0 \le \lambda_1(\theta) \le \cdots \le \lambda_m(\theta) \le \cdots \to \infty,$$

for all $m \ge 1$, $\lambda_m(\theta)$ is a Lipschitz's function of $\theta \in Y' =]-\pi, \pi]$.

The Bloch spectrum (Aguirre and Conca 1988; Conca and Vanninathan 1997) is defined as

$$\sigma_B = \{\lambda_m(\theta) : \theta \in Y', m \ge 1\} = \bigcup_{m \ge 1} \left[\min_{\theta \in Y'} \lambda_m(\theta), \max_{\theta \in Y'} \lambda_m(\theta) \right].$$

Also, for all $k \ge 1$, $\alpha_k = \lambda_k(0)$, $\beta_k = \lambda_k(\pi)$ and

$$\sigma_B = [\alpha_0, \beta_0] \cup [\beta_1, \alpha_1] \cup [\alpha_2, \beta_2] \cup [\beta_3, \alpha_3] \cup \cdots .$$

In particular, $\lambda_{2k-1}(0)$ is the minimum of $\lambda_{2k-1}(\theta)$, while $\lambda_{2k-1}(\pi)$is the maximum of $\lambda_{2k-1}(\theta)$, and $\lambda_{2k}(0)$ is the maximum of $\lambda_{2k}(\theta)$, while $\lambda_{2k}(\pi)$ is the minimum of $\lambda_{2k}(\theta)$.

Thus, we have a characterization for the region of stability S of the Hill's equation (1). The closure of the stability intervals are precisely the called *Bloch bands*, i.e.,

$$[\alpha_m, \beta_m] = \left[\min_{\theta\in Y'} \lambda_m(\theta), \max_{\theta\in Y'} \lambda_m(\theta)\right].$$

The non-empty open intervals between two Bloch bands are called *gaps*. Their union, together with the unbounded open interval below the first Bloch band, is exactly the unstable region U.

2.2 The exponential spectrum

In this section, we define the exponential spectrum of Eq. (1). Let us consider the following two spectral problems parameterized by $\theta \in \mathbb{R}$.

$$\begin{cases} \text{Find } \mu = \mu(\theta) \in \mathbb{R} \text{ and } \Psi = \Psi(x,\theta); \\ -\Psi''(x,\theta) + V(x)\Psi(x,\theta) = \mu(\theta)\Psi(x,\theta) \\ \Psi(x+1,\theta) = e^{\theta}\Psi(x,\theta), \quad \forall x. \end{cases} \tag{7}$$

$$\begin{cases} \text{Find } \nu = \nu(\theta) \in \mathbb{R} \text{ y } \Psi = \Psi(x,\theta); \\ -\Psi''(x,\theta) + V(x)\Psi(x,\theta) = \nu(\theta)\Psi(x,\theta) \\ \Psi(x+1,\theta) = -e^{\theta}\Psi(x,\theta), \quad \forall x. \end{cases} \tag{8}$$

We have the following results.

(i) For any $\theta \in \mathbb{R}$, there exists a minimal first eigenvalue μ_0 of (7) which is real, simple and such that $\theta \mapsto \mu_0(\theta)$ is analytic, concave and even. Also,

$$\begin{aligned} &\lim_{\theta\to+\infty} \mu_0(\theta) = -\infty \text{ and} \\ &\max_{\theta\in\mathbb{R}} \mu_0(\theta) = \mu_0(0) = \lambda_0(0) = \alpha_0. \end{aligned}$$

(ii) Assume that $\beta_{2k} \le \beta_{2k+1}$. Then there exists $\theta_{2k,2k+1} \ge 0$ such that, for $\theta \in]-\theta_{2k,2k+1}, \theta_{2k,2k+1}[$, there exist $\nu_{2k}(\theta)$, $\nu_{2k+1}(\theta)$ real and simple eigenvalues of (8) which satisfy $\theta \mapsto \nu_{2k}(\theta)$, $\nu_{2k+1}(\theta)$ are analytic and even, and $\nu_{2k}(\theta)$, $\nu_{2k+1}(\theta)$ are strictly monotone on $[0, \theta_{2k,2k+1}]$. Also,

$$\begin{aligned} &\min_{\theta\in[0,\theta_{2k,2k+1}]} \nu_{2k}(\theta) = \nu_{2k}(0) = \lambda_{2k}(\pi) = \beta_{2k}, \\ &\max_{\theta\in[0,\theta_{2k,2k+1}]} \nu_{2k+1}(\theta) = \nu_{2k+1}(0) = \lambda_{2k+1}(\pi) = \beta_{2k+1}, \\ &\lim_{|\theta|\to\theta_{2k,2k+1}} \nu_{2k}(\theta) = \lim_{|\theta|\to\theta_{2k,2k+1}} \nu_{2k+1}(\theta) = \nu_{2k,2k+1}, \\ &\{\nu_{2k}(\theta) : \theta \in [0, \theta_{2k,2k+1}]\} = [b_{2k}, \nu_{2k,2k+1}] \text{ and} \\ &\{\nu_{2k+1}(\theta) : \theta \in [0, \theta_{2k,2k+1}]\} = [\nu_{2k,2k+1}, b_{2k+1}]. \end{aligned}$$

(iii) Assume that $\alpha_{2k+1} \le \alpha_{2k+2}$. Then there exists $\theta_{2k+1,2k+2} \ge 0$ such that, for $\theta \in]-\theta_{2k+1,2k+2}, \theta_{2k+1,2k+2}[$, there exist $\mu_{2k+1}(\theta)$, $\mu_{2k+2}(\theta)$ real and simple eigenvalues of (7) which satisfy $\theta \mapsto \mu_{2k+1}(\theta)$, $\mu_{2k+2}(\theta)$ are analytic and even, and $\mu_{2k+1}(\theta)$, $\mu_{2k+2}(\theta)$ are strictly monotone on $[0, \theta_{2k+1,2k+2}]$. Also,

$$\begin{aligned} &\min_{\theta\in[0,\theta_{2k+1,2k+2}]} \mu_{2k+1}(\theta) = \mu_{2k+1}(0) = \lambda_{2k+1}(\pi) = \alpha_{2k+1}, \\ &\max_{\theta\in[0,\theta_{2k+1,2k+2}]} \mu_{2k+2}(\theta) = \mu_{2k+2}(0) = \lambda_{2k+2}(\pi) = \alpha_{2k+2}, \\ &\lim_{|\theta|\to\theta_{2k+1,2k+2}} \mu_{2k+1}(\theta) = \lim_{|\theta|\to\theta_{2k+1,2k+2}} \mu_{2k+2}(\theta) = \mu_{2k+1,2k+2}, \\ &\{\mu_{2k+1}(\theta) : \theta \in [0, \theta_{2k+1,2k+2}]\} = [a_{2k+1}, \mu_{2k+1,2k+2}] \text{ and} \\ &\{\mu_{2k+2}(\theta) : \theta \in [0, \theta_{2k+1,2k+2}]\} = [\mu_{2k+1,2k+2}, a_{2k+2}]. \end{aligned}$$

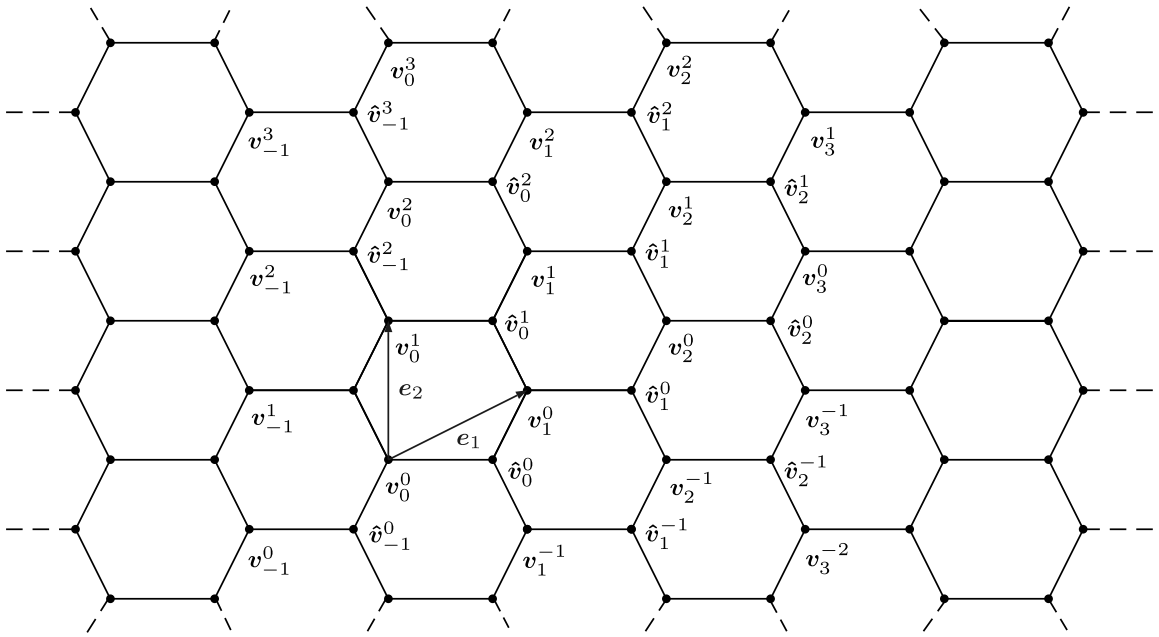

Fig. 2 Vertices $\boldsymbol{v}_i^j$ and $\hat{\boldsymbol{v}}_i^j$ representing the graphene G

Thus, the authors of Allaire and Orive (2005) conclude that

$$\mathbb{R} = \sigma_B \cup \sigma_e \quad \text{and} \quad \sigma_B \cap \sigma_e = \bigcup_{i=0}^{+\infty} \{\alpha_i\} \cup \{\beta_i\}, \tag{9}$$

where

$$\begin{aligned}\sigma_e = &\{\mu_0(\theta) : \theta \in \mathbb{R}\} \cup \{\mu_{2k+1}(\theta), \mu_{2k+2}(\theta) : \theta \in [0, \theta_{2k+1,2k+2}]\} \\ &\cup \{\nu_{2k}(\theta), \nu_{2k+1}(\theta) : \theta \in [0, \theta_{2k,2k+1}]\}.\end{aligned}$$

We can see that if $\varphi_1(\cdot;\lambda)$ is the function defined in (2), then there exists three sets, $\mathfrak{A}$, $\mathfrak{B}$ y $\mathfrak{C}$, such that

$$\lambda \in \mathfrak{A} \Leftrightarrow |\varphi_1(t;\lambda)| \leq 1, \ \forall t \in \mathbb{R}, \tag{10}$$

$$\lambda \in \mathfrak{B} \Leftrightarrow \varphi_1(t;\lambda) > 1, \quad \forall t \in \mathbb{R}, \tag{11}$$

$$\lambda \in \mathfrak{C} \Leftrightarrow \varphi_1(t;\lambda) < -1, \ \forall t \in \mathbb{R}. \tag{12}$$

3 The graphene

The graphene is a substance made of pure carbon, where the atoms follow a regular hexagon pattern. This atoms are mathematically described by a set of vertices $\mathcal{V} \subseteq \mathbb{R}^2$ as Fig. 2 shows.

More precisely, let us introduce the vectors

$$\boldsymbol{e}_1 = \left(\tfrac{3}{2}, \tfrac{\sqrt{3}}{2}\right) \quad \text{and} \quad \boldsymbol{e}_2 = \left(0, \sqrt{3}\right). \tag{13}$$

Then, the set of vertices $\mathcal{V}$ is defined by

$$\mathcal{V} = \left\{\boldsymbol{v}_i^j, \hat{\boldsymbol{v}}_i^j : i, j \in \mathbb{Z}\right\}, \tag{14}$$

where the family of vertices $(\boldsymbol{v}_i^j)_{i,j\in\mathbb{Z}}$ and $(\hat{\boldsymbol{v}}_i^j)_{i,j\in\mathbb{Z}}$ are defined by the relations:

$$\boldsymbol{v}_i^j = i\boldsymbol{e}_1 + j\boldsymbol{e}_2, \tag{15}$$

$$\hat{\boldsymbol{v}}_i^j = \boldsymbol{v}_i^j + (1, 0). \tag{16}$$

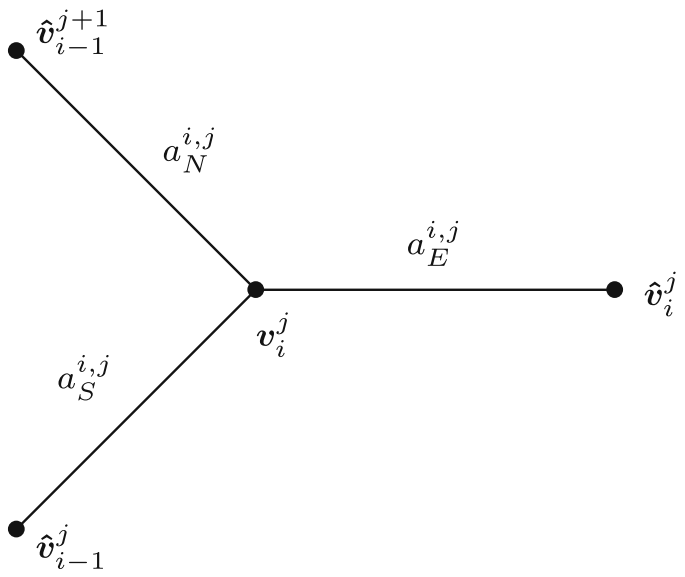

Fig. 3 Edges $a_E^{i,j}$, $a_N^{i,j}$ and $a_S^{i,j}$, and their respective vertices

As Fig. 2 shows, these vertices are connected by a set of edges $\mathcal{A}$ defined by

$$\mathcal{A} = \left\{a_E^{i,j}, a_N^{i,j}, a_S^{i,j} : a_E^{i,j} = [\boldsymbol{v}_i^j, \hat{\boldsymbol{v}}_i^j], a_N^{i,j} = [\boldsymbol{v}_i^j, \hat{\boldsymbol{v}}_{i-1}^j], a_S^{i,j} = [\boldsymbol{v}_i^j, \hat{\boldsymbol{v}}_{i-1}^{j+1}], i, j \in \mathbb{Z}\right\}, \tag{17}$$

as it is displayed in Fig. 3. These set of edges and vertices constitute an hexagonal grid.

Using this notation, the structure of the graphene is represented by a non-oriented graph G determined by the set of vertices and edges previously defined, i.e.,

$$G = (\mathcal{V}, \mathcal{A}).$$

We notice that each edge of the graphene is bijective to the segment $[0, 1] \subseteq \mathbb{R}$. In fact, to visualize this bijection, we consider the parameterization $\boldsymbol{\sigma}$, oriented from $\boldsymbol{v}$ to $\boldsymbol{w}$, defined by

$$\begin{aligned} \boldsymbol{\sigma} : [0, 1] \times \mathbb{R}^2 \times \mathbb{R}^2 &\to \mathbb{R}^2 \\ (t; \boldsymbol{v}, \boldsymbol{w}) &\mapsto \boldsymbol{\sigma}(t; \boldsymbol{v}, \boldsymbol{w}) = \boldsymbol{v} + t(\boldsymbol{w} - \boldsymbol{v}). \end{aligned} \tag{18}$$

Thus, each edge $[\boldsymbol{v}_1, \boldsymbol{v}_2] \in \mathcal{A}$ can be written as $\boldsymbol{\sigma}([0, 1]; \boldsymbol{v}_1, \boldsymbol{v}_2)$. The inverse function is such that

$$\mathbf{x} \in [\boldsymbol{v}_1, \boldsymbol{v}_2] \mapsto \boldsymbol{\sigma}^{-1}(\mathbf{x}; \boldsymbol{v}_1, \boldsymbol{v}_2) = \frac{\| \mathbf{x} - \boldsymbol{v}_1 \|}{\| \boldsymbol{v}_2 - \boldsymbol{v}_1 \|}. \tag{19}$$

Using the parametrization (18), whose inverse is (19), for each edge $[\boldsymbol{v}_1, \boldsymbol{v}_2] \in \mathcal{A}$ we can define the space $L^2(\boldsymbol{v}_1, \boldsymbol{v}_2)$ as follows:

$$L^2(\boldsymbol{v}_1, \boldsymbol{v}_2) = \left\{\widetilde{\Psi} \circ \boldsymbol{\sigma}^{-1}(\cdot; \boldsymbol{v}_1, \boldsymbol{v}_2) : \widetilde{\Psi} \in L^2(0, 1)\right\},$$

endowed with the norm $\|\widetilde{\Psi} \circ \boldsymbol{\sigma}^{-1}(\cdot; \boldsymbol{v}_1, \boldsymbol{v}_2)\|_{L^2(\boldsymbol{v}_1, \boldsymbol{v}_2)} = \|\widetilde{\Psi}\|_{L^2(0,1)}$. Then we can define $L^2(\mathcal{A})$ as

$$L^2(\mathcal{A}) = \left\{(\Psi_a)_{a \in \mathcal{A}} \in \bigoplus_{a \in \mathcal{A}} L^2(a) : \sum_{a \in \mathcal{A}} \|\Psi_a\|_{L^2(a)}^2 < \infty\right\}. \tag{20}$$

This space can be also called $L^2(G)$.

Similarly, for each edge $[\boldsymbol{v}_1, \boldsymbol{v}_2] \in \mathcal{A}$ we can define the Sobolev space $H^2(\boldsymbol{v}_1, \boldsymbol{v}_2)$ by

$$H^2(\boldsymbol{v}_1, \boldsymbol{v}_2) = \left\{\widetilde{\Psi} \circ \boldsymbol{\sigma}^{-1}(\cdot; \boldsymbol{v}_1, \boldsymbol{v}_2) : \widetilde{\Psi} \in H^2(0, 1)\right\},$$

endowed with the norm $\|\widetilde{\Psi} \circ \boldsymbol{\sigma}^{-1}(\cdot; \boldsymbol{v}_1, \boldsymbol{v}_2)\|_{H^2(\boldsymbol{v}_1,\boldsymbol{v}_2)} = \|\widetilde{\Psi}\|_{H^2(0,1)}$. Thus, the Sobolev space $H^2(G)$ is defined as the subset of functions $(\Psi_a)_{a\in\mathcal{A}} \in \bigoplus_{a\in\mathcal{A}} H^2(a)$ which satisfy the three following conditions:

$$\sum_{a\in\mathcal{A}} \|\Psi_a\|^2_{H^2(a)} < \infty, \tag{21}$$

$$\forall \boldsymbol{v} \in \mathcal{V}, \forall a_1, a_2 \in \mathcal{A}\, [\boldsymbol{v} \in a_1 \cap a_2 \Rightarrow \Psi_{a_1}(\boldsymbol{v}) = \Psi_{a_2}(\boldsymbol{v})], \tag{22}$$

$$\forall \boldsymbol{v} \in \mathcal{V} \sum_{\substack{\boldsymbol{v}_2\in\mathcal{V} \\ [\boldsymbol{v},\boldsymbol{v}_2]\in\mathcal{A}}} D\Psi_{[\boldsymbol{v},\boldsymbol{v}_2]}(\boldsymbol{v}; \boldsymbol{v}_2 - \boldsymbol{v}) = 0, \tag{23}$$

where we have denoted by $D\Psi_{[\boldsymbol{v},\boldsymbol{v}_2]}(\boldsymbol{v}; \boldsymbol{v}_2 - \boldsymbol{v})$ the directional derivative of the function $\Psi_{[\boldsymbol{v},\boldsymbol{v}_2]}$ at the point $\boldsymbol{v}$ in the direction $[\boldsymbol{v}_2 - \boldsymbol{v}]$. These conditions are usually called Neumann conditions of the graphene or Kirchhoff conditions. Equation (22) corresponds to the continuity condition on each vertex going from one edge to the other. It implies that the electron wavefunction is continuous throughout the lattice and its spatial derivative, related to the momentum of the electrons, is always well defined, a physically necessary condition. The second Eq. (23), states that the sum of the outward fluxes from the vertex $\boldsymbol{v}$ must be zero. This zero-fluxes condition for the wavefunction implies that the electrons in the lattice are not accumulating at the nodes. This is analogous to the zero sum of flows in a pipe network where an incompressible fluid circulates.

4 The Hamiltonian of graphene

Let us now define the Hamiltonian of graphene in $L^2(G)$. Let $V(t)$ be a function in $L^2(0, 1)$ such that

$$V(t) = V(1 - t). \tag{24}$$

The *Hamiltonian of graphene* $\mathcal{H} : \mathcal{D}(\mathcal{H}) \subset L^2(G) \to L^2(G)$ is the operator, with domain $\mathcal{D}(\mathcal{H}) = H^2(G)$, that maps $\Psi = (\Psi_a)_{a\in\mathcal{A}} \in H^2(G)$ to $\mathcal{H}\Psi \in L^2(G)$, $\mathcal{H}\Psi = ((\mathcal{H}\Psi)_a)_{a\in A}$, such that

$$(\mathcal{H}\Psi)_a(\mathbf{x}) = \left(-\widetilde{\Psi}_a'' + V\widetilde{\Psi}_a\right) \circ \boldsymbol{\sigma}^{-1}(\mathbf{x}; a), \tag{25}$$

where, for each edge $a \in \mathcal{A}$, $\widetilde{\Psi}_a = \Psi_a \circ \boldsymbol{\sigma}(\cdot; a) \in H^2(0, 1)$.

The goal of this section is to study the spectrum of the operator $\mathcal{H}$, characterizing the functions Ψ which are bounded or unbounded solutions. In order to do this, we seek for non-zero functions $\Psi = (\Psi_a)_{a\in\mathcal{A}}$ satisfying (22)–(23) and the following differential equations:

$$-\widetilde{\Psi}_a''(t) + V(t)\widetilde{\Psi}_a(t) = \lambda\widetilde{\Psi}_a(t), \quad \forall a \in \mathcal{A}, \forall t \in (0, 1), \tag{26}$$

where $\lambda \in \mathbb{R}$ is a parameter.

Our goal is to classify the solutions of (26) according to the different values of λ, looking for bounded and unbounded solutions of graphene. We see that the condition (21) is not satisfied by our solutions since the operator $\mathcal{H}$ has continuous spectrum.

We are interested in studying the solutions of (26) that satisfy the properties

$$\Psi(\mathbf{x} + \boldsymbol{e}_1) = R_1\Psi(\mathbf{x}), \forall \mathbf{x} \in G \tag{27}$$

$$\Psi(\mathbf{x} + \boldsymbol{e}_2) = R_2\Psi(\mathbf{x}), \forall \mathbf{x} \in G \tag{28}$$

where R_1 and R_2 are real or complex numbers belonging to the set

$$D_R = \{R \in \mathbb{C} : |R| = 1 \ \vee \ R \in \mathbb{R} - \{0\}\}.$$

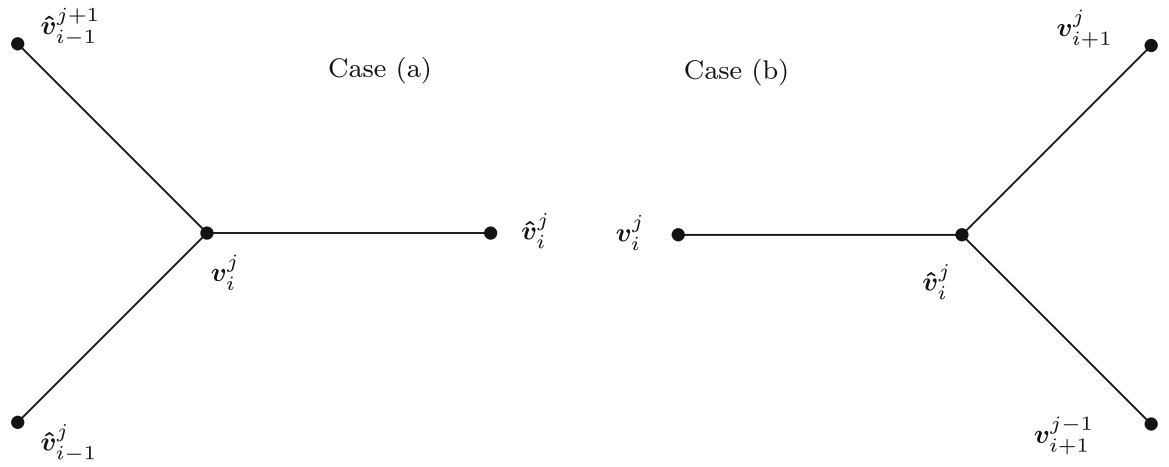

Fig. 4 Adjacent edges to the vertices of type $\hat{\boldsymbol{v}}_i^j$ (Case (a)) and type $\boldsymbol{v}_i^j$ (Case (b))

We notice that if $|R_1| = |R_2| = 1$, the solutions will be bounded in the graphene, whereas if one of the two constants has modulus different than one, the solution will be unbounded in the direction $\pm\boldsymbol{e}_1$ o $\pm\boldsymbol{e}_2$.

A periodic solution, of the type in Eqs. (27) and (28), is expected in a periodic system such as graphene, as a consequence of Bloch theorem (Bloch 1929). When the environment in which the electrons move around repeats periodically in space, like a crystal, the electrons wave function will have the same period as the crystal, a property common for all solid states systems with a crystalline lattice structure.

To study this situation we will proceed as follows: in Sect. 5, we will analyze how to impose Kirchhoff's conditions (22)–(23) and, in Sect. 6, we will characterize the values of λ respect to the constants R_1, R_2.

5 Kirchhoff's conditions

In this section, we will properly characterize the functions $\Psi = (\Psi_a)_{a\in\mathcal{A}}$ that satisfy Kirchhoff's conditions (22)–(23). First of all, we notice that each vertex $\boldsymbol{v} \in \mathcal{V}$ has exactly three adjacent edges, as Fig. 4 shows. Hence, continuity and flux conditions will be explicitly written at the vertices of type $\boldsymbol{v}_i^j$ and $\hat{\boldsymbol{v}}_i^j$ of $\mathcal{V}$, where $i, j \in \mathbb{Z}$ (see 14).

The main result in this section will be split in two theorems separating the cases $\varphi_2(1;\lambda) \neq 0$ and $\varphi_2(1;\lambda) = 0$, where $\varphi_2(\cdot;\lambda)$ is the function defined in (2). This separation is important because in the second case λ is included in the Dirichlet spectrum. The first theorem completely characterizes the functions that satisfy the flux and continuity conditions stated in (22)–(23).

Theorem 1 *If $\varphi_2(1;\lambda) \neq 0$, then every function $\Psi = (\Psi_a)_{a\in\mathcal{A}}$ satisfying* (26)*, also satisfies* (22)–(23) *if and only if, for each $i, j \in \mathbb{Z}$, it holds*

$$-3\varphi_1(1;\lambda)\Psi(\boldsymbol{v}_i^j) + \Psi(\hat{\boldsymbol{v}}_i^j) + \Psi(\hat{\boldsymbol{v}}_{i-1}^j) + \Psi(\hat{\boldsymbol{v}}_{i-1}^{j+1}) = 0, \tag{29}$$

$$-3\varphi_1(1;\lambda)\Psi(\hat{\boldsymbol{v}}_i^j) + \Psi(\boldsymbol{v}_i^j) + \Psi(\boldsymbol{v}_{i+1}^j) + \Psi(\boldsymbol{v}_{i+1}^{j-1}) = 0, \tag{30}$$

where $\varphi_1(\cdot;\lambda)$ and $\varphi_2(\cdot;\lambda)$ are the functions described in (2).

Theorem 2 *If $\varphi_2(1;\lambda)=0$, every function $\Psi=(\Psi_a)_{a\in\mathcal{A}}$ satisfying* (26)*, also satisfies the* (22)–(23) *if and only if the following conditions hold:*

(1) *There exists $k_\Psi\in\mathbb{R}$, depending on Ψ, such that*

$$\Psi(\boldsymbol{v}_i^j)=k_\Psi \quad \text{and} \quad \Psi(\hat{\boldsymbol{v}}_i^j)=k_\Psi\varphi_1(1;\lambda), \quad \forall i,\, j\in\mathbb{Z}. \tag{31}$$

(2) *If on each edge $a\in\mathcal{A}$, the functions Ψ_a can be written as*

$$\widetilde{\Psi}_a(t)=\widetilde{\Psi}_a(0)\varphi_1(t;\lambda)+c_a\varphi_2(t;\lambda), \tag{32}$$

where the parameterization t is chosen such that the edge goes from left to right, then the constants $(c_a)_{a\in\mathcal{A}}$ satisfy the relations:

$$2k_\Psi\varphi_1'(1;\lambda)+c_{[\hat{\boldsymbol{v}}_{i-1}^{j+1},\boldsymbol{v}_i^j]}+c_{[\hat{\boldsymbol{v}}_{i-1}^{j},\boldsymbol{v}_i^j]}=c_{[\boldsymbol{v}_i^j,\hat{\boldsymbol{v}}_i^j]}\varphi_1(1;\lambda), \quad \forall i,\, j\in\mathbb{Z}, \tag{33}$$

$$k_\Psi\varphi_1'(1;\lambda)+c_{[\boldsymbol{v}_i^j,\hat{\boldsymbol{v}}_i^j]}\varphi_1(1;\lambda)=c_{[\hat{\boldsymbol{v}}_i^j,\boldsymbol{v}_{i+1}^j]}+c_{[\hat{\boldsymbol{v}}_i^j,\hat{\boldsymbol{v}}_{i+1}^{j-1}]}, \quad \forall i,\, j\in\mathbb{Z}. \tag{34}$$

5.1 Proof of Theorem 1

We begin by enunciating the following lemma, where we introduce two auxiliary functions that will be used in this section.

Lemma 1 *If $\varphi_2(1;\lambda)\neq 0$, then there exist two solutions $\phi_1(\cdot;\lambda)$ and $\phi_2(\cdot;\lambda)$ of* (1) *that satisfy the boundary conditions*

$$\phi_1(0;\lambda)=1, \quad \phi_1(1;\lambda)=0, \tag{35}$$

and

$$\phi_2(0;\lambda)=0, \quad \phi_2(1;\lambda)=1. \tag{36}$$

Moreover, $\phi_1(\cdot;\lambda)$ and $\phi_2(\cdot;\lambda)$ are unique and are determined by

$$\phi_1(t;\lambda)=\varphi_1(t;\lambda)-\left(\frac{\varphi_1(1;\lambda)}{\varphi_2(1;\lambda)}\right)\varphi_2(t;\lambda), \tag{37}$$

$$\phi_2(t;\lambda)=\left(\frac{1}{\varphi_2(1;\lambda)}\right)\varphi_2(t;\lambda). \tag{38}$$

Proof Existence follows directly from evaluating (37)–(38) in $t=0$ and $t=1$. To prove uniqueness of $\phi_1(\cdot;\lambda)$, let us assume that there exists a function $\phi_{1b}(\cdot;\lambda)$ solution of (1) that satisfies (35). This solution can be written as a linear combination of $\varphi_1(\cdot;\lambda)$ and $\varphi_2(\cdot;\lambda)$ as follows

$$\phi_{1b}(t;\lambda)=c_1\varphi_1(t;\lambda)+c_2\varphi_2(t;\lambda).$$

Evaluating at $t=0$ and using (35) we obtain $c_1=1$. Now, by taking $t=1$, from (35) and (37), we get

$$-\left(\frac{\varphi_1(1;\lambda)}{\varphi_2(1;\lambda)}\right)\varphi_2(1;\lambda)=c_2\varphi_2(1;\lambda) \tag{39}$$

which leads to $c_2=-\left(\frac{\varphi_1(1;\lambda)}{\varphi_2(1;\lambda)}\right)$, i.e., $\phi_{1b}(t;\lambda)=\phi_1(t;\lambda)$. Uniqueness of $\phi_2(\cdot;\lambda)$ can be obtained similarly. □

Considering the functions $\phi_1(\cdot;\lambda)$ and $\phi_2(\cdot;\lambda)$ defined in Lemma 1, we can prove Theorem 1 as follows.

Proof of Theorem 1 The condition (22) is satisfied if and only if the function $\Psi = (\Psi_a)_{a\in\mathcal{A}}$ has a well-defined and unique trace (independent on the edge) on each vertex $\boldsymbol{v} \in \mathcal{V}$ of graphene. In expressions (29) and (30) , we have explicitly used the values of traces of u at each vertex of the form $\boldsymbol{v}_i^j, \hat{\boldsymbol{v}}_i^j \in \mathcal{V}$. To finish the proof, we focus on the flux property (23).

We will prove that the identity (29) is equivalent to the flux condition (23) at the vertices $\boldsymbol{v}_i^j$ of Fig. 4-Case (a). To simplify the notation, we denote by f, g and h to restrictions of the function u to the edges $[\boldsymbol{v}_i^j, \hat{\boldsymbol{v}}_{i-1}^{j+1}]$, $[\boldsymbol{v}_i^j, \hat{\boldsymbol{v}}_{i-1}^j]$ and $[\boldsymbol{v}_i^j, \hat{\boldsymbol{v}}_i^j]$, respectively; and by A, B, C and D, the traces of the function Ψ at the vertices $\boldsymbol{v}_i^j$, $\hat{\boldsymbol{v}}_{i-1}^{j+1}$, $\hat{\boldsymbol{v}}_{i-1}^j$ and $\hat{\boldsymbol{v}}_i^j$, respectively (see Fig. 5).

Since the function $\Psi = (\Psi_a)_{a\in\mathcal{A}}$ satisfies (26), its traces are well defined at the vertices and $\varphi_2(1;\lambda) \neq 0$, we can use the functions $\phi_1(\cdot;\lambda)$, $\phi_2(\cdot;\lambda)$ defined in (35)–(36) to find its values on each edge $[\boldsymbol{v}_i^j, \hat{\boldsymbol{v}}_{i-1}^{j+1}]$, $[\boldsymbol{v}_i^j, \hat{\boldsymbol{v}}_{i-1}^j]$ and $[\boldsymbol{v}_i^j, \hat{\boldsymbol{v}}_i^j]$ in terms of its corresponding values at the vertices as follows:

$$\begin{cases} \tilde{f}(t) = A\phi_1(t;\lambda) + B\phi_2(t;\lambda) \\ \tilde{g}(t) = A\phi_1(t;\lambda) + C\phi_2(t;\lambda) \\ \tilde{h}(t) = A\phi_1(t;\lambda) + D\phi_2(t;\lambda), \end{cases} \tag{40}$$

where $\tilde{f}$, $\tilde{g}$ and $\tilde{h}$ represent the composition of the functions f, g, h with the parameterization $\boldsymbol{\sigma}$ defined in (18) for each edge. With this notation, the condition (23) written at the vertex $\hat{\boldsymbol{v}}_i^j$ is equivalent to

$$\tilde{f}'(0) + \tilde{g}'(0) + \tilde{h}'(0) = 0. \tag{41}$$

Then taking derivatives in (40) and replacing in (41), we get

$$3A\phi_1'(0;\lambda) + (B + C + D)\phi_2'(0;\lambda) = 0. \tag{42}$$

The values $\phi_1'(0;\lambda)$ and $\phi_2'(0;\lambda)$ can be directly obtained by taking derivatives in the definitions (37)–(38), evaluating at $t = 0$ and using the properties (2). Thus, the identity (42) is equivalent to

$$-3A\left(\frac{\varphi_1(1;\lambda)}{\varphi_2(1;\lambda)}\right) + (B + C + D)\left(\frac{1}{\varphi_2(1;\lambda)}\right) = 0.$$

Multiplying this expression by $\varphi_2(1;\lambda)$, we finally obtain

$$-3A\varphi_1(1;\lambda) + B + C + D = 0,$$

which is exactly the identity (29) with the corresponding changes in nomenclature.

The proof for (30) is similar, since Eq. (30) is equivalent to the flux conditions (23) established at the vertices $\hat{\boldsymbol{v}}_i^j$ (Fig. 4-Case (b)). □

5.2 Proof of Theorem 2

In this section, we study the particular case where $\varphi_2(1;\lambda) = 0$. Since the function $\varphi_2(\cdot;\lambda)$ also vanishes at $t = 0$ (see 2), then $\varphi_2(\cdot;\lambda)$ is a non-trivial solution of the following Dirichlet boundary value problem:

$$\begin{cases} -\varphi_2''(x;\lambda) + V(x)\varphi_2(x;\lambda) = \lambda\varphi_2(x;\lambda), & \text{in } (0,1) \\ \varphi_2(0;\lambda) = \varphi_2(1;\lambda) = 0. \end{cases}$$

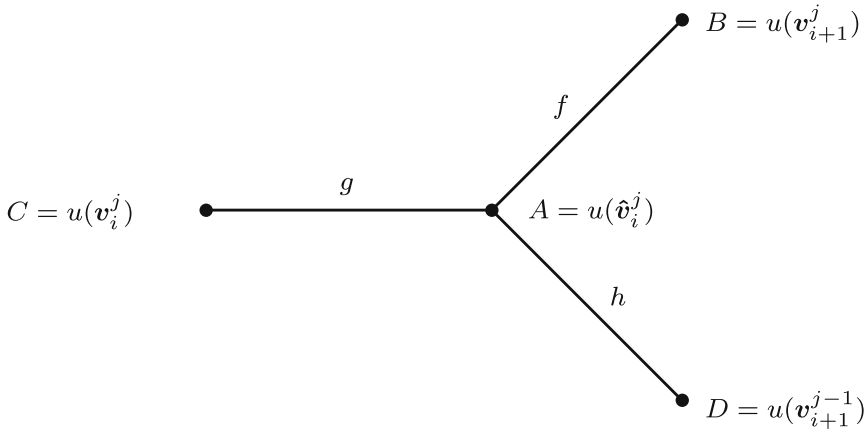

Fig. 5 Vertices where the values of function u are A, B, C and D

Hence, the case we are interested in this section corresponds to the values of λ of the spectrum of the Dirichlet operator associated with the differential operator $\mathcal{H}$.

In the following lemma, we summarize additional properties of the functions $\varphi_1(\cdot;\lambda)$ and $\varphi_2(\cdot;\lambda)$ that are satisfied in this case.

Lemma 2 *If* $\varphi_2(1;\lambda) = 0$, *then*

$$\begin{aligned} &\varphi_2'(1;\lambda) = \varphi_1(1;\lambda) = 1 \quad \textit{and} \;\; \mathcal{D}(\lambda) = 2, \;\; \textit{or} \\ &\varphi_2'(1;\lambda) = \varphi_1(1;\lambda) = -1 \;\; \textit{and} \;\; \mathcal{D}(\lambda) = -2, \end{aligned}$$

where $\mathcal{D}(\lambda)$ *has been defined in* (5).

Proof From (24), we have that $\varphi_1(1-t;\lambda)$ and $\varphi_2(1-t;\lambda)$ are solutions of (1) and, therefore, they can be written as a linear combination of $\varphi_1(\cdot;\lambda)$ and $\varphi_2(\cdot;\lambda)$ as follows:

$$\varphi_1(1-t;\lambda) = \varphi_1(1;\lambda)\varphi_1(t;\lambda) - \varphi_1'(1;\lambda)\varphi_2(t;\lambda), \tag{43}$$

$$\varphi_2(1-t;\lambda) = \varphi_2(1;\lambda)\varphi_1(t;\lambda) - \varphi_2'(1;\lambda)\varphi_2(t;\lambda). \tag{44}$$

Considering $t = 1$ in (43) and in the derivative of (44), we have

$$\begin{aligned} 1 &= \varphi_1(1;\lambda)^2 - \varphi_1'(1;\lambda)\varphi_2(1;\lambda) \\ -1 &= \varphi_2(1;\lambda)\varphi_1'(1;\lambda) - \varphi_2'(1;\lambda)^2, \end{aligned}$$

i.e.,

$$\varphi_1'(1;\lambda)\varphi_2(1;\lambda) = \varphi_1(1;\lambda)^2 - 1, \tag{45}$$

$$\varphi_1'(1;\lambda)\varphi_2(1;\lambda) = \varphi_2'(1;\lambda)^2 - 1. \tag{46}$$

From (45)–(46), we have

$$\varphi_2'(1;\lambda)^2 = \varphi_1(1;\lambda)^2 = 1 \tag{47}$$

and, from (4), we conclude

$$\varphi_2'(1;\lambda) = \varphi_1(1;\lambda) = 1, \;\text{ or }\; \varphi_2'(1;\lambda) = \varphi_1(1;\lambda) = -1.$$

Thus, from (5),

$$\mathcal{D}(\lambda) = 2, \;\text{ or }\; \mathcal{D}(\lambda) = -2,$$

respectively. □

Proof of Theorem 2 To show part (1), we consider an arbitrary edge $a = [\boldsymbol{v}_1, \boldsymbol{v}_2] \in \mathcal{A}$ joining the vertices $\boldsymbol{v}_1, \boldsymbol{v}_2$. Since Ψ satisfies (26), from (3), we can write

$$\widetilde{\Psi}_{[\boldsymbol{v}_1,\boldsymbol{v}_2]}(t) = \widetilde{\Psi}_{[\boldsymbol{v}_1,\boldsymbol{v}_2]}(0)\varphi_1(t;\lambda) + \widetilde{\Psi}'_{[\boldsymbol{v}_1,\boldsymbol{v}_2]}(0)\varphi_2(t;\lambda), \quad \forall t \in [0,1].$$

Since $\varphi_2(1;\lambda) = 0$, we get

$$\widetilde{\Psi}_{[\boldsymbol{v}_1,\boldsymbol{v}_2]}(1) = \widetilde{\Psi}_{[\boldsymbol{v}_1,\boldsymbol{v}_2]}(0)\varphi_1(1;\lambda),$$

that is,

$$\Psi(\boldsymbol{v}_2) = \Psi(\boldsymbol{v}_1)\varphi_1(1;\lambda). \tag{48}$$

Since this relation is true on each edge and $\varphi_1(1;\lambda)^2 = 1$, we conclude that going through two consecutive edges $[\boldsymbol{v}_1, \boldsymbol{v}_2]$–$[\boldsymbol{v}_2, \boldsymbol{v}_3]$ there holds $\Psi(\boldsymbol{v}_3) = \Psi(\boldsymbol{v}_1)$. Then using the notation $k_\Psi = \Psi(\boldsymbol{v}_0^0)$ and noticing that all the vertices $\boldsymbol{v}_i^j$ are connected by the union of two consecutive edges, we get that

$$\Psi(\boldsymbol{v}_i^j) = k_\Psi \qquad \forall i, j \in \mathbb{Z}.$$

Thus, (31) is obtained using this identity together with (48) which allows us to relate the vertices $\boldsymbol{v}_i^j$ with $\hat{\boldsymbol{v}}_i^j$.

To prove (33), we study the flux condition on the vertices of type $\boldsymbol{v}_i^j \in \mathcal{V}$. To simplify notation, we denote by f, g and h, the restriction of the function Ψ to the edges $[\hat{\boldsymbol{v}}_{i-1}^{j+1}, \boldsymbol{v}_i^j]$, $[\hat{\boldsymbol{v}}_{i-1}^j, \boldsymbol{v}_i^j]$ and $[\boldsymbol{v}_i^j, \hat{\boldsymbol{v}}_i^j]$, respectively, and by A, the trace of the function Ψ on the central vertex $\boldsymbol{v}_i^j$ (see Fig. 6). Using (48), we obtain that the traces of Ψ on the external vertices $\hat{\boldsymbol{v}}_{i-1}^{j+1}$, $\hat{\boldsymbol{v}}_{i-1}^j$ and $\hat{\boldsymbol{v}}_i^j$, are equal to $A\varphi_1(1;\lambda)$. To use the notation in (32), we denote by c_f, c_g and c_h the corresponding constants $c_{[\hat{\boldsymbol{v}}_{i-1}^{j+1}, \boldsymbol{v}_i^j]}$, $c_{[\hat{\boldsymbol{v}}_{i-1}^j, \boldsymbol{v}_i^j]}$ and $c_{[\boldsymbol{v}_i^j, \hat{\boldsymbol{v}}_i^j]}\varphi_1(1;\lambda)$.

Then using (32), we write

$$\begin{cases} \tilde{f}(t) = A\varphi_1(1;\lambda)\ \varphi_1(t;\lambda) + c_f\ \ \varphi_2(t;\lambda) \\ \tilde{g}(t) = A\varphi_1(1;\lambda)\ \varphi_1(t;\lambda) + c_g\ \ \varphi_2(t;\lambda) \\ \tilde{h}(t) = \qquad A \qquad \varphi_1(t;\lambda) + c_h\ \ \varphi_2(t;\lambda), \end{cases} \tag{49}$$

where $\tilde{f}$, $\tilde{g}$ and $\tilde{h}$ represent the composition of f, g, h with the parameterization $\boldsymbol{\sigma}$ defined in (18) for each edge.

Thus, the flux condition (23) on the vertex $\boldsymbol{v}_i^j$ can be written as

$$-\tilde{f}'(1) - \tilde{g}'(1) + \tilde{h}'(0) = 0. \tag{50}$$

Hence, taking derivative in (49) and replacing in (50), from (2), we get

$$2A\varphi_1(1;\lambda)\varphi_1'(1;\lambda) + (c_f + c_g)\varphi_2'(1;\lambda) = c_h.$$

Multiplying by $\varphi_1(1;\lambda)$ and using (4) and (47), we conclude that

$$2A\varphi_1'(1;\lambda) + c_f + c_g = c_h\varphi_1(1;\lambda).$$

We have proved, with corresponding changes of notation, that the flux condition (23) written at the vertex $\boldsymbol{v}_i^j$ is equivalent to the identity (33).

Similarly, we can prove that the flux condition (23) written at the vertex $\hat{\boldsymbol{v}}_i^j$ is equivalent to the identity (34).

Thus, the conditions (22)–(23) are satisfied if and only if the identities (31), (33) and (34) are also satisfied. □

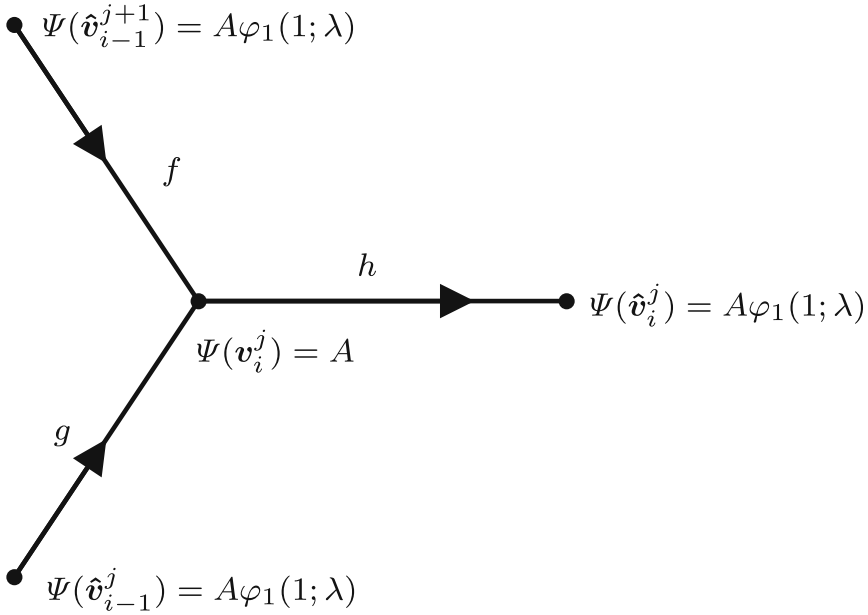

Fig. 6 Vertices where the function u is A and $A\varphi_1(1;\lambda)$, and the respective orientation of the parameterization t

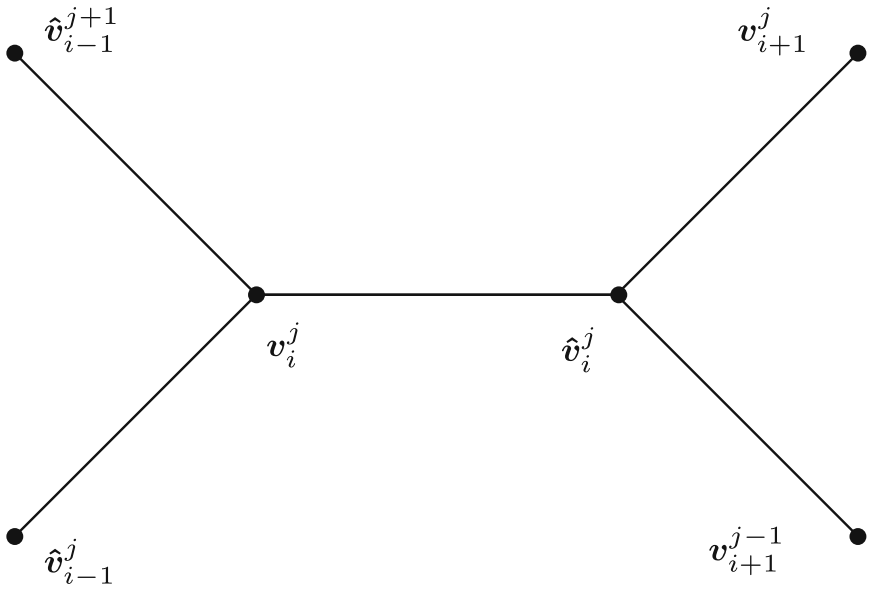

Fig. 7 Vertices $\boldsymbol{v}_i^j$ and $\hat{\boldsymbol{v}}_i^j$ and their corresponding adjacent vertices

6 Spectral theory in the graphene

In this section, we are interested in characterizing all functions $\Psi = (\Psi_a)_{a\in\mathcal{A}}$ that satisfy (26), the continuity and flux conditions (22)–(23), and also the quasi-periodicity conditions (27)–(28). The analysis in this section is restricted to the case where the values $\lambda \in \mathbb{R}$ satisfy $\varphi_2(1;\lambda) \neq 0$.

We will use the result shown in Theorem 1, applied to the vertices $\boldsymbol{v}_i^j$ and $\hat{\boldsymbol{v}}_i^j$, for all $i, j \in \mathbb{Z}$ (see Fig. 7).

From definitions (15)–(16), it holds that

$$\begin{aligned} \boldsymbol{v}_i^j &= \boldsymbol{v}_{i+1}^j - \boldsymbol{e}_1, \quad \boldsymbol{v}_{i+1}^{j-1} = \boldsymbol{v}_{i+1}^j - \boldsymbol{e}_2 \\ \hat{\boldsymbol{v}}_i^j &= \hat{\boldsymbol{v}}_{i-1}^j + \boldsymbol{e}_1, \quad \hat{\boldsymbol{v}}_{i-1}^{j+1} = \hat{\boldsymbol{v}}_{i-1}^j + \boldsymbol{e}_2. \end{aligned}$$

Hence, properties (27)–(28) transform the identities (29)–(30) to

$$\begin{aligned} -3\varphi_1(1;\lambda)\Psi(\boldsymbol{v}_i^j) + \left(1 + R_1^{-1} + R_1^{-1}R_2\right)\Psi(\hat{\boldsymbol{v}}_i^j) = 0, \\ -3\varphi_1(1;\lambda)\Psi(\hat{\boldsymbol{v}}_i^j) + \left(1 + R_1 + R_1R_2^{-1}\right)\Psi(\boldsymbol{v}_i^j) = 0. \end{aligned}$$

If we multiply the first equation by R_1 and reorder the system leaving as variables the quantities $R_1\Psi(\boldsymbol{v}_i^j)$ and $\Psi(\hat{\boldsymbol{v}}_i^j)$, we get

$$-3\varphi_1(1;\lambda)R_1\Psi(\boldsymbol{v}_i^j) + \left(1 + R_1 + R_2\right)\Psi(\hat{\boldsymbol{v}}_i^j) = 0, \tag{51}$$

$$\left(1 + R_1^{-1} + R_2^{-1}\right)R_1\Psi(\boldsymbol{v}_i^j) - 3\varphi_1(1;\lambda)\Psi(\hat{\boldsymbol{v}}_i^j) = 0. \tag{52}$$

These identities allow us to obtain the solutions in terms of λ, R_1 and R_2, as a homogeneous linear system of equations. Thus, we conclude that it as a non-trivial solution if and only if the determinant of the corresponding matrix is zero, i.e., if

$$9\varphi_1(1;\lambda)^2 = (1 + R_1 + R_2)(1 + R_1^{-1} + R_2^{-1}). \tag{53}$$

Equation (53) constitutes the dispersion relation of graphene for bounded or unbounded solutions having the quasi-periodic behavior (27)–(28). This equation relates the type of functions we seek, represented by the constants R_1 and R_2 (wave type), with the values of $\lambda \in \mathbb{C}$ (frequencies) through the function $\varphi_1(1;\lambda)$.

In the following sections, we will investigate for which values of λ bounded or unbounded solutions of the problem are obtained.

6.1 Bounded solutions

In this section, we study the dispersion relation (53) in the case where R_1 and R_2 are such that the solution $\Psi = (\Psi_a)_{a\in\mathcal{A}}$ is bounded. Clearly, R_1 and R_2 must satisfy $|R_1| = |R_2| = 1$.

For this analysis, it is convenient to introduce the auxiliary variables $\theta_1, \theta_2 \in [-\pi, \pi]$ such that

$$R_1 = e^{i\theta_1} \qquad R_2 = e^{i\theta_2}. \tag{54}$$

In this way, the dispersion relation of graphene (53) becomes

$$9\varphi_1(1;\lambda)^2 = (1 + e^{i\theta_1} + e^{i\theta_2})(1 + e^{-i\theta_1} + e^{-i\theta_2}). \tag{55}$$

Noticing here that the right-hand side is the product of a complex number and its conjugate, we can write

$$\varphi_1(1;\lambda)^2 = F(\theta_1, \theta_2) := \tfrac{1}{9}\left|1 + e^{i\theta_1} + e^{i\theta_2}\right|^2. \tag{56}$$

Simple calculations show that

$$0 \le F(\theta_1, \theta_2) \le 1, \quad \forall \theta_1, \theta_2 \in [-\pi, \pi].$$

In addition,

$$\left\{F(\theta_1, \theta_2) : \theta_1, \theta_2 \in [-\pi, \pi]\right\} = [0, 1].$$

This result is summarized in the following lemma.

Lemma 3 *For each $\theta_1, \theta_2 \in [-\pi, \pi]$, the solutions $\varphi_1(1;\lambda)$ of* (26) *that satisfy* (2) *also satisfy*

$$\varphi_1(1;\lambda) \in [-1, 1].$$

This result, together with the theory developed in Sect. 2, implies the following corollary.

Corollary 1 *For each $\theta_1, \theta_2 \in [-\pi, \pi]$, the values of λ associated with the solutions $\varphi_1(1;\lambda)$ of* (26) *that satisfy* (2) *are given by*

$$\lambda \in \varphi_1^{-1}\left(\sqrt{F(\theta_1,\theta_2)}\right) \cup \varphi_1^{-1}\left(-\sqrt{F(\theta_1,\theta_2)}\right),$$

where φ_1^{-1} denotes the preimage set of the function $\varphi_1(1;\lambda)$.

Remark 1 From (10), (11) and (12), it follows that

$$\lambda \in \mathfrak{A}_\theta \cup \mathfrak{A}_{\pi-\theta},$$

where

$$\theta = \cos^{-1}\sqrt{F(\theta_1,\theta_2)}$$

and the sets $\mathfrak{A}_\theta$ are defined by

$$\mathfrak{A}_\theta = \{\lambda_i(\theta) : i \in \mathbb{N}\}.$$

6.2 Unbounded solutions

We study now the dispersion relation (53) when $R_1, R_2 \in \mathbb{R}^*$. In this case, the expression on the right-hand side can have different values for different R_1 and R_2. That is why we are interested in characterizing the regions:

$$\mathcal{R}_S = \left\{(R_1, R_2) \in \mathbb{R}^2 : 0 \le (1 + R_1 + R_2)(1 + R_1^{-1} + R_2^{-1}) < 9\right\} \tag{57}$$

$$\mathcal{R}_U = \left\{(R_1, R_2) \in \mathbb{R}^2 : 9 \le (1 + R_1 + R_2)(1 + R_1^{-1} + R_2^{-1})\right\}. \tag{58}$$

We will show Theorem 3.

Remark 2 We are not interested in the analysis in the region $(1+R_1+R_2)(1+R_1^{-1}+R_2^{-1}) < 0$, because in this case the system (51)–(52) does not have a non-trivial solution.

Theorem 3 *The regions $\mathcal{R}_S$ and $\mathcal{R}_U$ defined in* (57)–(58) *are not empty. Moreover, they are characterized by* (see Fig. 8)

(i) *If $R_1, R_2 > 0$, then $(R_1, R_2) \in \mathcal{R}_U$.*
(ii) *If $R_2 \in (-\infty, -1)$, then*

$$(R_1, R_2) \in \mathcal{R}_S \iff R_1 \in \left[\frac{-R_2}{1+R_2}, R_{1,2}\right) \cup [-(1+R_2), R_{1,1})$$
$$(R_1, R_2) \in \mathcal{R}_U \iff R_1 \in [R_{1,2}, 0) \cup [R_{1,1}, +\infty).$$

(iii) *If $R_2 = -1$, then $(R_1, R_2) \in \mathcal{R}_S$.*

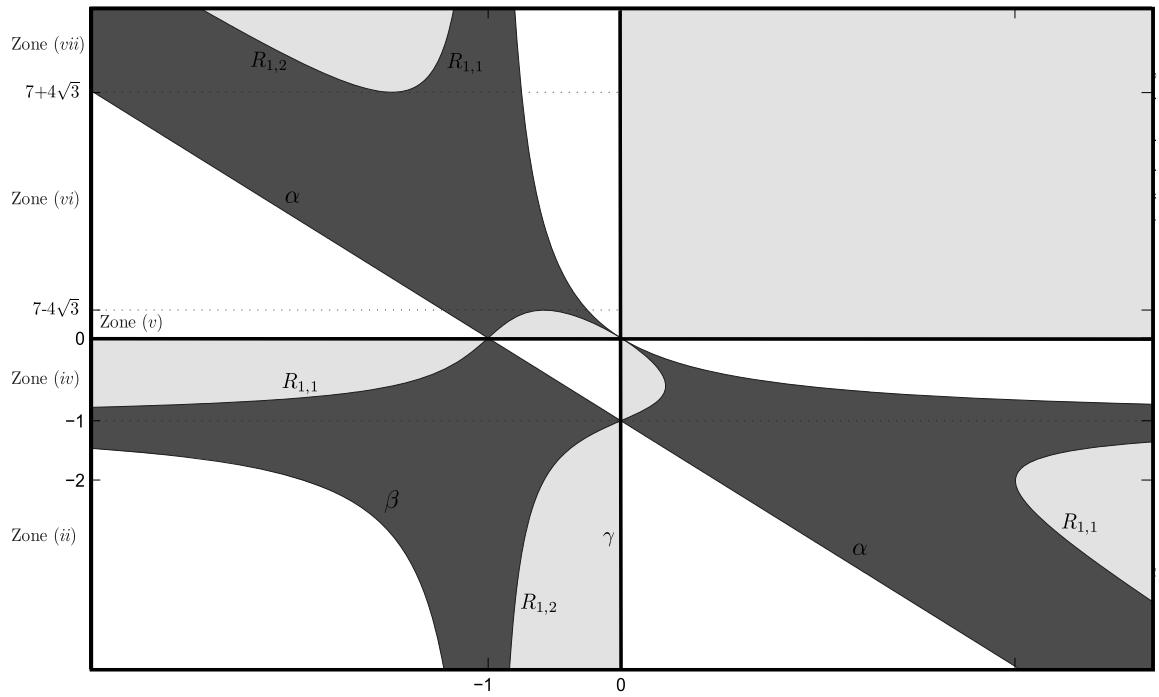

Fig. 8 Regions $\mathcal{R}_S$ (red) and $\mathcal{R}_U$ (yellow), separated by the curves $\alpha : R_1 = -(1+R_2)$, $\beta : R_1 = \dfrac{-R_2}{1+R_2}$, $\gamma : R_1 = 0$, $R_1 = R_{1,1}$ and $R_1 = R_{1,2}$. The white regions are not interesting (see Remark 2)

(iv) *If* $R_2 \in (-1, 0)$, *then*

$$\begin{aligned}(R_1, R_2) \in \mathcal{R}_S &\iff R_1 \in (R_{1,1}, -(1+R_2)] \cup \left(R_{1,2}, \frac{-R_2}{1+R_2}\right]\\ (R_1, R_2) \in \mathcal{R}_U &\iff R_1 \in (-\infty, R_{1,1}] \cup (0, R_{1,2}].\end{aligned}$$

(v) *If* $R_2 \in (0, 7-4\sqrt{3})$, *then*

$$\begin{aligned}(R_1, R_2) \in \mathcal{R}_S &\iff R_1 \in [-(1+R_2), R_{1,1}) \cup \left(R_{1,2}, \frac{-R_2}{1+R_2}\right]\\ (R_1, R_2) \in \mathcal{R}_U &\iff R_1 \in [R_{1,1}, R_{1,2}] \cup (0, +\infty).\end{aligned}$$

(vi) *If* $R_2 \in [7-4\sqrt{3}, 7+4\sqrt{3}]$, *then*

$$\begin{aligned}(R_1, R_2) \in \mathcal{R}_S &\iff R_1 \in \left[-(1+R_2), \frac{-R_2}{1+R_2}\right]\\ (R_1, R_2) \in \mathcal{R}_U &\iff R_1 \in (0, \infty).\end{aligned}$$

(vii) *If* $R_2 \in (7+4\sqrt{3}, \infty)$, *then*

$$\begin{aligned}(R_1, R_2) \in \mathcal{R}_S &\iff R_1 \in [-(1+R_2), R_{1,2}) \cup \left(R_{1,1}, \frac{-R_2}{1+R_2}\right]\\ (R_1, R_2) \in \mathcal{R}_U &\iff R_1 \in [R_{1,2}, R_{1,1}] \cup (0, +\infty).\end{aligned}$$

In (ii), (iv), (v) and (vii), $R_{1,1}$ *and* $R_{1,2}$ *are given by*

$$R_{1,1} = -\left(\frac{R_2^2 - 6R_2 + 1}{2(R_2+1)}\right) + \frac{(R_2-1)\sqrt{R_2^2 - 14R_2 + 1}}{2(R_2+1)}$$
$$R_{1,2} = -\left(\frac{R_2^2 - 6R_2 + 1}{2(R_2+1)}\right) - \frac{(R_2-1)\sqrt{R_2^2 - 14R_2 + 1}}{2(R_2+1)}.$$

Proof To show (i), it is enough to notice that

$$(1 + R_1 + R_2)(1 + R_1^{-1} + R_2^{-1}) = 3 + (R_1 + R_1^{-1}) + (R_2 + R_2^{-1}) + \left(\frac{R_1}{R_2} + \left(\frac{R_1}{R_2}\right)^{-1}\right).$$

Thus, if $R_1, R_2 > 0$, each term in parenthesis of the right-hand side is greater or equal than two; hence, $(R_1, R_2) \in \mathcal{R}_U$.

To study the other cases, let us begin by characterizing those points that belong to $\mathcal{R}_U \cup \mathcal{R}_S$, i.e., those points in the plane that satisfy

$$G_1(R_1, R_2) := (1 + R_1 + R_2)(1 + R_1^{-1} + R_2^{-1}) \geq 0. \tag{59}$$

First, it is convenient to reorder the expression $G_1(R_1, R_2)$ from (59) as follows:

$$G_1(R_1, R_2) = \frac{(R_1 + R_2 + 1)(R_1(R_2+1) + R_2)}{R_1 R_2}.$$

Here the numerator is a quadratic expression when $R_2 \neq -1$. In this case, $G_1(R_1, R_2)$ changes sign at the points

$$-(1 + R_2), \quad \frac{-R_2}{1 + R_2}, \quad 0$$

and, towards $-\infty$, has the same sign as $\frac{R_2+1}{R_2}$. With this information, we can solve inequality (59) for R_2 in different intervals:

$$\text{If } R_2 < -1, \text{ it holds } R_1 \in \left[\frac{-R_2}{1+R_2}, 0\right) \cup [-(1+R_2), \infty). \tag{60}$$

$$\text{If } R_2 \in (-1, 0), \text{ it holds } R_1 \in (-\infty, -(1+R_2)] \cup \left(0, \frac{-R_2}{1+R_2}\right]. \tag{61}$$

$$\text{If } R_2 > 0, \text{ it holds } R_1 \in \left[-(1+R_2), \frac{-R_2}{1+R_2}\right] \cup (0, \infty). \tag{62}$$

If $R_2 = -1$, inequality (59) becomes

$$G_1(R_1, -1) := 1 \geq 0, \tag{63}$$

which is valid for all $R_1 \in \mathbb{R}^*$.

To find the separation between the regions $\mathcal{R}_S$ and $\mathcal{R}_U$, it is enough to find the solution to the inequality

$$G_2(R_1, R_2) := (1 + R_1 + R_2)(1 + R_1^{-1} + R_2^{-1}) - 9 \geq 0,$$

which is equivalent to

$$G_2(R_1, R_2) = \frac{1}{R_1 R_2}\left(R_1^2(R_2+1) + R_1(R_2^2 - 6R_2 + 1) + R_2(R_2+1)\right) \geq 0. \tag{64}$$

Once again, the case $R_2 = -1$ can be isolated and (64) becomes

$$G_2(R_1, R_2) = -8 \geq 0,$$

which is false for all $R_1 \in \mathbb{R}^*$. This, together with (63), implies (iii).

In the general case $R_2 \neq -1$, if we factor out $R_2 + 1$ in (64), we have

$$G_2(R_1, R_2) = \frac{R_2 + 1}{R_1 R_2}\left(R_1^2 + R_1 \frac{R_2^2 - 6R_2 + 1}{R_2 + 1} + R_2\right). \tag{65}$$

Then to solve inequality (64), we can see that it is convenient to factorize the quadratic expression

$$R_1^2 + R_1 \frac{R_2^2 - 6R_2 + 1}{R_2 + 1} + R_2, \tag{66}$$

whose discriminant is

$$\triangle = \frac{(R_2 - 1)^2(R_2^2 - 14R_2 + 1)}{(R_2 + 1)^2} = \frac{(R_2 - 1)^2\Big(R_2 - (7 + 4\sqrt{3})\Big)\Big(R_2 - (7 - 4\sqrt{3})\Big)}{(R_2 + 1)^2}.$$

Thus, if $R_2 \in [7 - 4\sqrt{3}, 7 + 4\sqrt{3}] \subseteq \mathbb{R}^+$, the quadratic expression (66) is always greater or equal than zero, and then inequality (64) is equivalent to

$$\frac{1}{R_1} \geq 0, \tag{67}$$

whose solution belong to $(0, \infty)$. This, together with (62), implies (vi).

If $R_2 \notin [7 - 4\sqrt{3}, 7 + 4\sqrt{3}]$, the quadratic (66) can be written as

$$(R_1 - R_{1,1})(R_1 - R_{1,2}),$$

where $R_{1,1}$ and $R_{1,2}$ are given by

$$R_{1,1} = -\left(\frac{R_2^2 - 6R_2 + 1}{2(R_2 + 1)}\right) + \frac{(R_2 - 1)\sqrt{R_2^2 - 14R_2 + 1}}{2(R_2 + 1)},$$
$$R_{1,2} = -\left(\frac{R_2^2 - 6R_2 + 1}{2(R_2 + 1)}\right) - \frac{(R_2 - 1)\sqrt{R_2^2 - 14R_2 + 1}}{2(R_2 + 1)}.$$

Hence, we can factorize (65) as follows:

$$G_2(R_1, R_2) = \frac{R_2 + 1}{R_1 R_2}(R_1 - R_{1,1})(R_1 - R_{1,2}).$$

In this case, $G_2(R_1, R_2)$ changes sign at the points

$$R_{1,1}, \quad R_{1,2}, \quad 0$$

and, towards $-\infty$, has the same sign as $\frac{R_2+1}{R_2}$. Using this information we can solve inequality (64) for R_2 in different intervals as follows:

If $R_2 < -1$, it holds that $R_1 \in [R_{1,2}, 0) \cup [R_{1,1}, +\infty)$,

If $R_2 \in (-1, 0)$, it holds that $R_1 \in (-\infty, R_{1,1}] \cup (0, R_{1,2}]$,

If $R_2 \in (0, 7 - 4\sqrt{3})$, it holds that $R_1 \in [R_{1,1}, R_{1,2}] \cup (0, +\infty)$,

If $R_2 > 7 + 4\sqrt{3}$, it holds that $R_1 \in [R_{1,2}, R_{1,1}] \cup (0, +\infty)$.

Comparing this result and (60)–(61), we obtain the cases (ii), (iv), (v) and (vii). □

Remark 3 From (10), (11) y (12), the following cases hold:

- If $(R_1, R_2) \in \mathcal{R}_S$, then $\lambda \in \mathfrak{A}_\theta \cup \mathfrak{A}_{\pi-\theta}$, with $\theta = \cos^{-1}\sqrt{G(\theta_1,\theta_2)} \in (0, \pi/2]$
- If $(R_1, R_2) \in \mathcal{R}_U$, then $\lambda \in \mathfrak{B}_\theta \cup \mathfrak{C}_\theta$, with $\theta = \cosh^{-1}\sqrt{G(\theta_1,\theta_2)} \in (0, \infty)$.

Here the sets $\mathfrak{A}_\theta$, $\mathfrak{B}_\theta$ and $\mathfrak{C}_\theta$ are defined by

$$\mathfrak{A}_\theta = \{\lambda_i(\theta) : i \in \mathbb{N}\},\ \mathfrak{B}_\theta = \{\mu_i(\theta) : i \in \mathbb{N}\},\ \mathfrak{C}_\theta = \{\nu_i(\theta) : i \in \mathbb{N}\},$$

where $\lambda_i(\theta)$, $\mu_i(\theta)$ and $\nu_i(\theta)$ are the eigenvalues mentioned in problems (6), (7) and (8), respectively, and the function G is given by

$$G(\theta_1,\theta_2) = \frac{1}{9}(1 + R_1 + R_2)(1 + R_1^{-1} + R_2^{-1}).$$

Remark 4 The eigenvectors obtained for each value of $\lambda = \lambda(R_1, R_2)$ satisfy (51) and (53). Then it values at the vertices $(\boldsymbol{v}_i^j)$ and $(\hat{\boldsymbol{v}}_i^j)$ satisfy the relation

$$\Psi(\hat{\boldsymbol{v}}_i^j) = \pm R_1\sqrt{\frac{1 + R_1^{-1} + R_2^{-1}}{1 + R_1 + R_2}}\,\Psi(\boldsymbol{v}_i^j). \tag{68}$$

Using (27)–(28) and (68), we obtain that the eigenvectors are characterized by

$$\Psi(\boldsymbol{v}_i^j) = R_1^i R_2^j \Psi(\boldsymbol{v}_0^0),$$
$$\Psi(\hat{\boldsymbol{v}}_i^j) = \pm R_1^{i+1} R_2^j \sqrt{\frac{1 + R_1^{-1} + R_2^{-1}}{1 + R_1 + R_2}}\,\Psi(\boldsymbol{v}_0^0).$$

7 Conclusions

We solved the eigenvalues problem for the Hamiltonian of the electron wave function in graphene considering Kirchhoff conditions, characterizing the stability of the solution.

Knowing that the spectrum of the Hill equation (1) can be completely characterized in one dimension by (9), we looked for an analogous result for the spectrum of the Hamiltonian $\mathcal{H}$, defined in (25), in the hexagonal network G for graphene.

We divided the problem into two cases depending on the boundary condition: Dirichlet conditions when one of the basis functions of the Hill equation is equal to zero, $\varphi_2(1, \lambda) = 0$; and a non-trivial case otherwise, $\varphi_2(1, \lambda) \neq 0$. The analysis of both cases led us to the two main theorems of this work 1 and 2, respectively.

We obtained bounded solutions when considering normalized imaginary characteristic multipliers (54), which are two-dimensional analogs of the one-dimensional Bloch spectrum. We explicitly obtained the dispersion relation of the problem (53). From this, we verified that the basis function $\varphi_1(1; \lambda)$ is greater than minus one and less than one, as established by the Lemma 3. Thus, this result coincides with the theory developed in one dimension (Allaire and Orive 2005). However, when we consider real characteristic multipliers, $R_1, R_2 \in \mathbb{R}^*$, the analogy breaks down. In one dimension, all the solutions are unstable, while in graph G, we obtained different regions where the solutions can be stable or unstable depending upon the eigenvalues. These regions are completely defined as indicated in Theorem 3 and the spectrum of $\mathcal{H}$ is completely determined.

Acknowledgements C. Conca and J. San Martín were partially supported from PFBasal-01 (CeBiB), PFBasal-03 (CMM) projects. C.Conca also received partial support from Ecos-Conicyt Grant C13E05 and by Fondecyt Grant 1140773. J. San Martín also received partial support from Fondecyt Grant 1180781. V. Solano was partially supported by Scholarship Program of CONICYT-Chile, Folio Number 21110749, by PFBasal-03 (CMM) project and by the Grants SEV-2011-0087 from Ministerio de Ciencia e Innovación (MICINN) of Spain. We would like to thank M. Solano for valuable comments on the manuscript.

References

Aguirre F, Conca C (1988) Eigenfrequencies of a tube bundle immersed in a fluid. Appl Math Optim 18(1):1–38
Alexander S (1983) Superconductivity of networks. A percolation approach to the effects of disorder. Phys Rev B 27(3):1541
Allaire G, Orive R (2005) On the band gap structure of Hill's equation. J Math Anal Appl 306(2):462–480
Amovilli C, Leys FE, March NH (2004) Electronic energy spectrum of two-dimensional solids and a chain of c atoms from a quantum network model. J Math Chem 36(2):93–112
Avron JE, Raveh A, Zur B (1988) Adiabatic quantum transport in multiply connected systems. Rev Mod Phys 60(4):873
Bloch F (1929) Über die quantenmechanik der elektronen in kristallgittern. Z Phys 52(7–8):555–600
Conca C, Planchard J, Vanninathan M (1995) Fluids and periodic structures. Wiley, Chichester
Conca C, Vanninathan M (1997) Homogenization of periodic structures via bloch decomposition. SIAM J Appl Math 57(6):1639–1659
Eastham MS (1973) The spectral theory of periodic differential equations. Scottish Academic Press, Edinburgh
De Gennes PG (1981) Champ critique d'une boucle supraconductrice ramefieé. C R Acad Sci Paris 292B:279–282
Harris PJF (2002) Carbon nano-tubes and related structures: new materials for the twenty-first century. AAPT
Katsnelson MI (2007) Graphene: carbon in two dimensions. Mater Today 10(1):20–27
Korotyaev E, Lobanov I (2006) Zigzag periodic nanotube in magnetic field. arXiv:math/0604007 (arXiv preprint)
Korotyaev E, Lobanov I (2007)Schrödinger operators on zigzag nanotubes. In: Annales henri poincare, vol 8, no 6. Birkhuser-Verlag, pp 1151–1176
Kuchment P (2002) Graph models for waves in thin structures. Waves Rand Media 12(4):R1–R24
Kuchment P (2004) Quantum graphs and their applications in special issue of waves in random media 14(1):S107–S128
Kuchment P, Post O (2007) On the spectra of carbon nano-structures. Commun Math Phys 275(3):805–826
Leys FE, Amovilli C, March NH (2004) Topology, connectivity and electronic structure of C and B cages and the corresponding nanotubes. J Chem Inf Comput Sci 44(1):122–135
Mills RGJ, Montroll EW (1970) Quantum theory on a network. II. A solvable model which may have several bound states per node point. J Math Phys 11(8):2525–2538
Montroll EW (1970) Quantum theory on a network. I. A solvable model whose wavefunctions are elementary functions. J Math Phys 11(2):635–648
Pauling L (1936) The diamagnetic anisotropy of aromatic molecules. J Chem Phys 4(10):673–677
Ruedenberg K, Scherr CW (1953) Free-electron network model for conjugated systems. I. Theory. J Chem Phys 21(9):1565–1581
Saito R, Dresselhaus G, Dresselhaus MS (1998) Physical properties of carbon nanotubes. World Scientific, Singapore